

CapST: An Enhanced and Lightweight Method for Deepfake Video Classification

Wasim Ahmad, Yan-Tsung Peng *Member, IEEE*, Yuan-Hao Chang *Fellow, IEEE*, Gaddisa Olani Ganfure, Sarwar Khan, Sahibzada Adil Shahzad

Abstract—The proliferation of deepfake videos, synthetic media produced through advanced Artificial Intelligence techniques, has raised significant concerns across various sectors, encompassing realms such as politics, entertainment, and security. In response, this research introduces an innovative and streamlined model designed to classify deepfake videos generated by five distinct encoders adeptly. Our approach not only achieves state-of-the-art performance but also optimizes computational resources. At its core, our solution employs part of a VGG19_bn as a backbone to efficiently extract features, a strategy proven effective in image-related tasks. We integrate a Capsule Network coupled with a Spatial-Temporal attention mechanism to bolster the model's classification capabilities while conserving resources. This combination captures intricate hierarchies among features, facilitating robust identification of deepfake attributes. Delving into the intricacies of our innovation, we introduce an existing video-level fusion technique that artfully capitalizes on temporal dependencies embedded within deepfake videos. By aggregating insights across frames, our model gains a holistic comprehension of video content, resulting in more precise predictions. Experimental results on an extensive benchmark dataset of deepfake videos (DFDM) showcase the efficacy of our proposed method. Notably, our approach achieves up to a 4% improvement in accurately categorizing deepfake videos compared to baseline models, all while demanding fewer computational resources.

Index Terms—Efficient DeepFake Detection Model (DFDM), Capsule Network, Dynamic Routing Algorithm (DRA), GAN's, Spatial-Temporal Attention (STA).

Wasim Ahmad is with the Institute of Information Science, Academia Sinica, Taipei 11529, Taiwan (R.O.C) and Department of Computer Science, National Chengchi University, Taipei 116, Taiwan (R.O.C) and Social Networks Human-Centered Computing, Taiwan International Graduate Program, Academia Sinica, Taipei 11529, Taiwan (R.O.C) (E-mail: was_last@iis.sinica.edu.tw)

Yan-Tsung Peng is with Department of Computer Science National Chengchi University, Taipei 116, Taiwan (R.O.C)(E-mail: yt-peng@cs.nccu.edu.tw).

Yuan-Hao Chang is with the Institute of Information Science, Academia Sinica, Taipei 11529, Taiwan (R.O.C) (E-mail: johnson@iis.sinica.edu.tw).

Gaddisa O.G. is with Dire Dawa University, Ethiopia (E-mail: gaddisaalex@gmail.com).

Sarwar Khan is with the Research Center for Information Technology Innovation, Academia Sinica, Taipei 11529, Taiwan (R.O.C) and Department of Computer Science, National Chengchi University, Taipei 116, Taiwan (R.O.C) and Social Networks Human-Centered Computing, Taiwan International Graduate Program, Academia Sinica, Taipei 11529, Taiwan (R.O.C) (E-mail: sarwar@iis.sinica.edu.tw).

Sahibzada Adil Shahzad is with the Institute of Information Science, Academia Sinica, Taipei 11529, Taiwan (R.O.C) and Department of Computer Science, National Chengchi University, Taipei 116, Taiwan (R.O.C) and Social Networks Human-Centered Computing, Taiwan International Graduate Program, Academia Sinica, Taipei 11529, Taiwan (R.O.C) (E-mail: adil-shah275@iis.sinica.edu.tw).

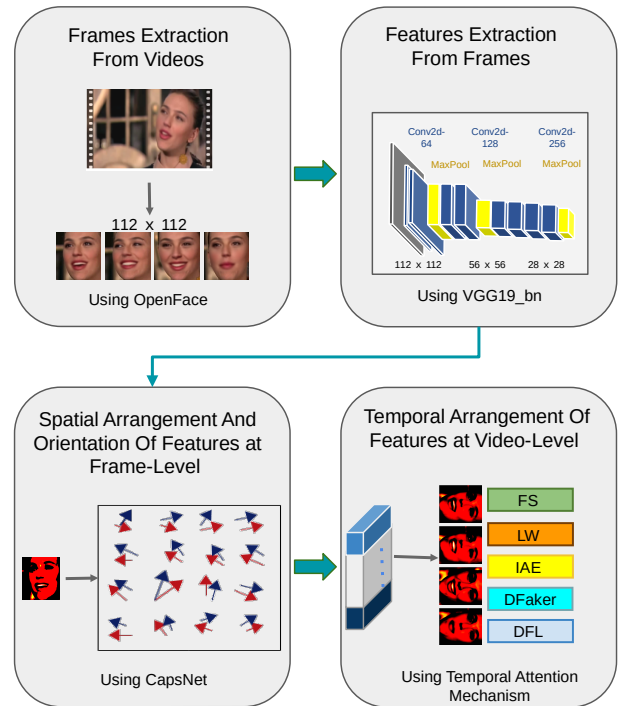


Fig. 1. General Overview of CapST. First, we extract the distinctive attributes of a set of video frames using VGG19_bn. Subsequently, these resultant features are fed into the capsule module to delineate spatial configurations within each frame. At last, these refined features are directed into the video-level fusion module, thereby enabling the classification of the manipulated class to which the video pertains.

I. INTRODUCTION

SIGNIFICANT advancements in computer hardware, particularly the introduction of powerful GPUs and TPUs, have greatly enhanced the performance of Artificial Intelligence (AI) algorithms. These algorithms have been widely utilized to solve various research problems across different domains. While these powerful hardware resources have proven invaluable for processing large artificial neural networks designed for complex problems, there needs to be more emphasis on developing lightweight artificial networks that consume fewer hardware resources while maintaining or improving the baseline performance. As hardware technologies progress, AI neural networks have evolved in size and complexity. Table I provides a comprehensive overview of the evolution of artificial neural networks in size and parameters. Similarly, II illustrates the varying number of parameters popular AI

networks utilize on state-of-the-art (SOTA) datasets. Although researchers in the field of AI primarily prioritize performance, regardless of the hardware resources required, the increasing resource demands have become a major concern for many institutions and individuals with limited resources who aim to progress in their research domains. Numerous contributions in this regard have been made by researchers throughout the years, proposing different efficient models to address this issue, including [1, 2, 3, 4, 5, 6], whose outstanding contributions enabled us not only to improve the performance over certain datasets but also reduces the sizes of the model intelligently. While we have discussed various models and their sizes on different state-of-the-art (SOTA) datasets, numerous datasets within each domain with unique characteristics require an efficient model that performs well while consuming fewer resources. Deepfake technology, combining elements of fake news and deep learning, has introduced various applications, such as Generative Adversarial Networks as depicted in 2. Generative Adversarial Networks (GANs) are a category of machine learning models comprising a pair of neural networks: the generator and the discriminator. The primary objective of the generator is to produce synthetic data resembling authentic data, whereas the discriminator is designed to distinguish between genuine and generated data. These two networks engage in competitive training, and over time, the generator becomes increasingly proficient at generating data that closely resembles reality. While GANs can generate images, they are not directly used for manipulating videos. However, variations of GANs are designed for video manipulation tasks. One such approach is video-to-video synthesis, where GANs convert videos from one domain to another. For example, it can be used to change a person’s appearance in a video from a source person to a target person. The process typically involves the following steps:

Collecting a dataset of paired videos, where each video in the source domain has a corresponding video in the target domain (e.g., videos of the same scene or activity but with different people). Training a video-to-video synthesis GAN on the paired dataset to learn the mapping between the two domains. Using the trained GAN to generate videos with the appearance of the target person while preserving the underlying activity from the source video.

It’s important to note that GANs are not the only technique used for video manipulation tasks. Other methods, such as optical flow-based approaches and pose-based methods, can also be used for similar tasks. In summary, GANs themselves are not directly used for video manipulation, but there are specialized variants of GANs and other techniques that can perform video-to-video synthesis and manipulate videos by replacing a source person with a target person. These manipulated videos pose a significant challenge in distinguishing between real and fake content with the naked eye. Consequently, this has raised concerns among prominent individuals globally, as false news spread or the synthesis of videos and images can harm and erode trust in social and electronic media.

In recent decades, significant efforts have been made to detect deepfake content. Despite advancements in detection techniques, evolving deepfake methods continuously challenge

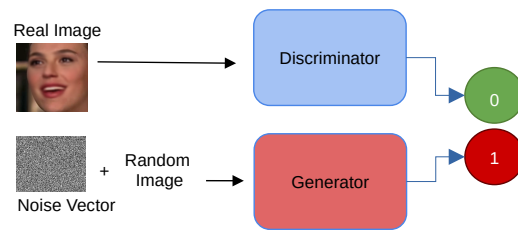


Fig. 2. The process of Generative Adversarial Networks (GANs) to produce lifelike and top-notch data involves training two neural networks, specifically a generator and a discriminator, within an adversarial framework.

detection. Diverse deepfake datasets, spanning voice, images, and videos, have been generated using advanced AI models. Detection methods primarily fall into two categories: one trains a model on genuine and manipulated data, classifying instances as "Real" or "Fake." Another method, as proposed by [7], manipulates original videos using five encoders, enhancing outcomes. Yet, there’s room for improved performance and resource efficiency. We have achieved significant advancements in addressing these challenges. Firstly, we reduced training and processing resources for the DFDM dataset. Our model outperforms the baseline [7] by up to 4%, marking substantial progress. Utilizing capsule networks, we introduced a spatial attention mechanism, offering benefits like hierarchical representation and pose estimation. Additionally, our method employs video-level fusion with a temporal attention mechanism, processing a limited number of frames to classify the entire video. Figure 1 illustrates our approach, CapST, using a constrained frame selection, VGG19_bn feature extraction, capsule modules, and video-level fusion for accurate classification. The subsequent sections of this article are organized as follows: Section II introduces the background of DeepFake Neural Networks and examines related works. In Section III, we present the architecture of our model in detail. Subsequently, in Section IV, we showcase the results obtained from our extensive experiments. Sections V and VI involve thorough discussions and analysis of our study’s findings. At last, in Section VII, we conclude our work, summarizing the significant contributions and insights gained from this research endeavor.

II. BACKGROUND AND RELATED WORK

A. Why are AI Models usually dense?

Artificial Intelligence (AI) models have become increasingly complex and resource-intensive over the past few years. These models are characterized by their high density and resource requirements, posing challenges to their deployment and practical implementation. In this literature review, we explore the reasons behind the dense nature of AI models and the factors contributing to their resource consumption.

Model Complexity and Performance: One primary reason for the dense nature of AI models is their increasing complexity. Deep learning architectures, such as convolutional neural networks (CNNs) or recurrent neural networks (RNNs), consist of multiple layers with numerous parameters [8]. These

TABLE I
EVOLUTION OF ARTIFICIAL NEURAL NETWORKS IN TERMS OF SIZES AND PARAMETERS (GENERAL OVERVIEW)

Evolutionary Stage	Network Characteristics	Parameter Size
Early Years	Small networks with a few layers and neurons	Limited number of manually set parameters
Feedforward Networks	Larger networks with increased depth and neurons per layer	more parameters as networks grow in size
Convolutional Neural Networks	Specialized for image processing, with convolution layers	Millions of parameters for complex image analysis
Recurrent Neural Networks	Designed for sequential data, such as time series or NLP	Varied parameter size based on specific architecture
Deep Neural Networks	Networks with many hidden layers for abstract representations	Millions to billions of parameters
Transformer Networks	Self-attention mechanisms for language processing tasks	Billions of parameters in recent state-of-the-art models

TABLE II
PARAMETER SIZES OF POPULAR DNNs ON DIFFERENT SOTA DATASETS

Dataset	Network	Params(M)
ImageNet	AlexNet	Around 60
	VGG16	Around 138
	ResNet50	Around 25
	InceptionV3	Around 23
	DenseNet121	Around 8
CIFAR-10	LeNet-5	Around 0.06
	VGG-like	Around 6
	ResNet20	Around 0.27
	DenseNet40	Around 0.35
MNIST	LeNet-5	Around 0.06
	VGG-like	Around 0.7
	MLP	Around 0.5

complex models can capture intricate patterns and achieve superior performance in various tasks, including image recognition, natural language processing, and speech synthesis [9, 10]. However, It comes at a price of increased model size and computational requirements. Capacity for Representation: Dense AI models aim to learn and represent vast information from the input data. They are designed to capture intricate features and relationships within the data, leading to improved accuracy and generalization [11]. The large number of parameters in these models allows them to approximate complex functions and extract high-level representations [12]. However, this capacity for representation contributes to their density and resource-intensive nature. Training on Large Datasets: AI models often require extensive training on large datasets to learn from diverse examples and generalize well. The availability of massive labeled datasets, such as ImageNet and COCO, has facilitated the training of deep learning models with millions or even billions of parameters [9]. Training on such large-scale datasets helps improve the model's ability to recognize and generalize patterns. However, this necessitates a significant amount of computational resources, including high-performance GPUs or specialized hardware accelerators [13]. Overparameterization and Optimization: The overparameterization of AI models, where the number of parameters exceeds the actual degrees of freedom in the problem, has been shown to enhance their optimization and generalization capabilities [14]. However, overparameterized models are inherently dense

and require additional computational resources during training and inference [15]. Techniques like regularization and pruning aim to mitigate the negative impact of overparameterization [14, 16]. However, these models remain resource-intensive. Model Compression and Deployment Challenges: The dense nature of AI models presents challenges in deployment and real-world implementation. Large model sizes make it difficult to deploy AI systems on resource-constrained devices such as smartphones, edge devices, or Internet of Things (IoT) devices [17]. Model compression techniques, including quantization, pruning, and knowledge distillation, have been proposed to reduce the model size and improve efficiency [14, 18, 19, 20]. However, these techniques often come at the cost of slight performance degradation. AI models' denseness and resource requirements can be attributed to their complexity, representation capacity, training on large datasets, overparameterization, and optimization techniques.

B. Popular Deepfake models and Datasets

Deepfake technology has made significant progress in recent years, driven by the development of sophisticated models and the availability of curated datasets. These models and datasets have played a crucial role in pushing the boundaries of deepfake synthesis, detection, and analysis. As discussed earlier, numerous studies have been proposed in the form of some outstanding AI models that outperformed on different datasets, as shown in the below section, but the issues with most of these models are primarily their size and complexity, which increase the demand of resources on a daily basis. This section will describe some famous deepfake detection models and datasets, along with the parameters they would consume.

1) *DeepFake Models*: XceptionNet [21] is a deep convolutional neural network architecture with a strong performance in deepfake detection tasks. It leverages depthwise separable convolutions to capture fine-grained features and has demonstrated high accuracy in distinguishing between genuine and manipulated facial videos. DeepFakeTIMIT [22] is a deepfake model specifically designed for audio-visual deepfake synthesis. It combines audio and visual information to create realistic deepfake content. Ensemble Models models combine the predictions of multiple deep-learning models to improve the overall detection performance. By leveraging the diversity of different models, ensemble models can achieve higher accuracy and robustness in deepfake detection

tasks. This approach often involves training several models independently and aggregating their predictions using voting or averaging techniques. SqueezeNAS [23] is an automated design framework for compact deepfake detection models. It utilizes neural architecture search techniques to efficiently explore the model design space and optimize for accuracy and computational efficiency. FWA-Net is a deepfake detection model that focuses on detecting facial warping artifacts. It leverages a two-stream architecture to learn features from spatial and temporal domains to identify manipulations in facial videos. Capsule-Forensics [24] proposed to utilize capsule networks, a type of neural network architecture that models hierarchical relationships between image features for detecting forged images and videos, including deepfakes. MesoNet [25] is a lightweight CNN-based model designed to detect manipulated facial videos at the mesoscopic level. It operates on low-resolution frames to identify artifacts indicative of deepfake manipulation. DFDNet [26] is a deepfake detection model that employs a two-stream architecture, incorporating both appearance and motion information from frames. It uses a combination of convolutional and recurrent layers to capture spatiotemporal features for accurate detection.

2) *Datasets*: FaceForensics++ [21] is considered a benchmark dataset for deepfake detection research, which comprises over 1,000 videos with manipulated facial content. It offers a diverse set of deepfake examples created using various methods. CelebA [27] was not explicitly developed for deepfake research but is a widely used dataset containing a large-scale collection of over 200,000 celebrity images. It is a valuable resource for training deepfake models, providing real-face images for comparison. DFDC (DeepFake Detection Challenge) Dataset [28] dataset was specifically curated for the DeepFake Detection Challenge, which aimed to advance the state-of-the-art performance in detecting deepfake videos. It includes thousands of real and deepfake videos for research and evaluation purposes. Face2Face [29] Dataset contains videos of individuals with their facial expressions manipulated to match another person's. It serves as a resource for studying facial expression transfer and deepfake techniques. VoxCeleb Dataset [30] is a large-scale audio-visual dataset with diverse celebrity speech data. While not designed specifically for deepfake research, it can be utilized for audio-visual deepfake synthesis and analysis. DeepfakeTIMIT [22] Dataset is tailored for audio-visual deepfake synthesis, utilizing the popular TIMIT dataset. It enables research on deepfake synthesis involving both audio and visual modalities. FBDB (Facebook Deepfake Detection Dataset) [31] is a large-scale dataset developed by Facebook for deepfake detection research. It contains a diverse collection of real and deepfake videos, providing a valuable resource for training and evaluating deepfake detection models.

C. Recent Deepfake Models and their parameters sizes

Although numerous contributions have been made in the last two decades on the issue of deepfake content, both on their generation and detection, as summarized in the above section in detail, some more recent and powerful AI techniques are utilized to overcome this issue in certain ways by designing

TABLE III
POPULAR DF MODELS, DATASETS AND ITS PARAMETERS

Models	Datasets			Params(M)
X-Ray [32]	FF++	UADFV	CDF_v1,v2	20.8
CNN+RNN [33]	FF++	UADFV	CDF_v1,v2	36
TSN [34]	FF++	UADFV	CDF_v1,v2	26.6
DSP-FWA [35]	FF++	UADFV	CDF_v1,v2	21.4
Two-stream [36]	FF++	UADFV	CDF_v1,v2	23.9
Meso4 [25]	FF++	UADFV	CDF_v1,v2	28.0
MesoInception4 [25]	FF++	UADFV	CDF_v1,v2	28.6
FWA [37]	FF++	UADFV	CDF_v1,v2	25.6
Xception-raw [21]	FF++	UADFV	CDF_v1,v2	22.9
Xception-c23 [21]	FF++	UADFV	CDF_v1,v2	22.9
Xception-c40 [21]	FF++	UADFV	CDF_v1,v2	22.9
Capsule [24]	FF++	UADFV	CDF_v1,v2	3.9
Multi-attentional [38]	FF++	UADFV	CDF_v1,v2	19.5
FTCN [34]	FF++	UADFV	CDF_v1,v2	26.6
RealForensics [35]	FF++	UADFV	CDF_v1,v2	21.4
ResVit [39]	FF++	DFD	CDF_v1,v2	21.4
Cross Eff_ViT [40]		DFDC		109
ViT distillation [41]		DFDC		373
Selim EffNet B7 [42]		DFDC		462
Convolutional ViT [43]		DFDC		89
Lipsync Matters [44]		FakeAVCeleb		35.97
Multimodal [45]		FakeAVCeleb		33.6

and proposing different model architectures. Some of them have performed amazingly well but at the cost of utilizing an enormous amount of resources in terms of parameters, as shown in Table III. Although it also depends on the size of the dataset how many videos it contains, how many different manipulated classes are generated from it, and different compression levels, etc., however, it is the responsibility of researchers to ensure the efficiency of their model to not only improve results but also take fewer resources.

D. Model Attribution

Model attribution involves the identification of the specific model employed to generate a synthetic image or video [46]. In the realm of image manipulation, the widespread use of GAN models has led to several investigations [47, 48, 49, 46, 50] into GAN model attribution for counterfeit images. These methodologies seek to extract distinct artificial markers left by diverse GAN models and engage in multi-class classification to ascribe the GAN model. Nevertheless, prior to [7], no preceding research has concentrated on model attribution for Deepfake face-swap videos. Although GAN models can produce Deepfakes, their effectiveness is often confined to controlled settings with uniform lighting conditions [31]. As a result, most publicly available face-swap Deepfakes are generated using Deepfake Autoencoder (DFAE) techniques. The feasibility of distinguishing between various DFAE models for Deepfake attribution and the applicability of image-based GAN model attribution techniques to DFAE models in the video domain remain subjects of exploration. These inquiries play a pivotal role in propelling advancements in Deepfake model attribution.

III. CAPST ARCHITECTURE

When proposing a Deep Neural Network (DNN) tailored to a specific domain, carefully considering resource utilization

TABLE IV
STRUCTURE OF DFDM DATASET [7]

Model	Input	Output	Encoder	Decoder	Variation
Faceswap (baseline)	64	64	4Conv+1Ups	3Ups+1Conv	/
Lightweight	64	64	3Conv+1Ups	3Ups+1Conv	Encoder
IAE	64	64	4Conv	4Ups+1Conv	Intermediate layers; Shared Encoder Decoder
Dfaker	64	128	4Conv+1Ups	3Ups+3Residual+1Conv	Decoder
DFL-H128	128	128	4Conv+1Ups	3Ups+1Conv	Input Resolution

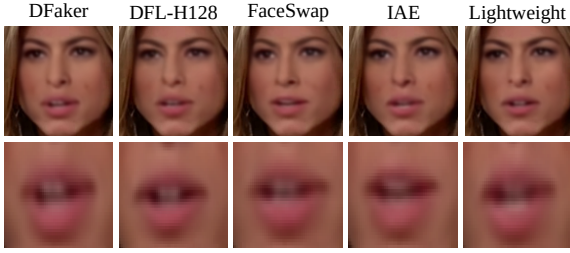


Fig. 3. DFDM Example: generated by different encoders

becomes paramount. While this study primarily focuses on minimizing network size regarding parameters and training time, our investigation centers on addressing deepfake content using DNNs. In this section, we outline the comprehensive architecture of our proposed CapST Model, delineating its diverse components. To explore the consistency and detectability of artifacts across varied Deepfakes, we introduce a novel and lightweight technique called CapST. This approach harmonizes the Capsule Network with Spatial (frame-level) and Temporal (video-level) attention mechanisms to extract discerning features. Algorithm 1 unveils the complexity of deepfake artifacts through a multi-stage process. It initiates by extracting frames from videos and deriving features via a VGG_19_bn network. These features are then fed into a Capsule Network module featuring Max Feature Map (MFM) Activation, Statistical Pooling, and Spatial Attention layers. The features are then concatenated and employ a Temporal Attention Map (TAM) for adaptable feature aggregation across frames. By synergistically employing these components, the algorithm aims to uncover deepfake attributes and elevate classification accuracy.

A. Unveiling the intricacies of DF artifacts at frame-level

The architecture of our CapST model is depicted in Figure 4. We first extract N number of faces from each video in the dataset, i.e.,

$$V_i = I_{f1}, I_{f2}, \dots, I_{fN}, \quad (1)$$

where V_i represents the input video while I_{f1}, \dots, I_{fN} represents the number of input frames we chose to consider for each video. After that, we pass these frames one by one to the VGG_19 network, where we extract the features of the input frame. We choose VGG_19bn [10] as a feature extractor pre-trained on [51] from the first-to-third Max-Pooling layer with a total of 26 layers. VGG_19bn is used as its performance is better throughout all the experiments than other CNN networks

in this specific task. The extracted features are then passed through the Capsule Network as shown in Figure 5.

We divided each primary capsule into three sections, including the Max Feature Map (MFM) [52] Activation function with the combination of Batch Normalization and Spatial Attention Layer, statistical pooling layer, and a 1-dimensional CNN. The statistical pooling layer is considered efficacious for forensics tasks and can improve the performance of the network [53, 54] by making the network independent even if the dimension of the input images vary. This is why it is argued that this network is not task-oriented and can be applied to different tasks without redesigning the whole network from scratch.

The capsule module first passes the input features through the MFM activation function proposed in [52], which enables the network to become light and robust as it suppresses the low activation neurons in each primary capsule. The output of the MFM is then passed through a spatial attention layer to aggregate the frame features [55]. The Statistical pooling layer is then used to calculate the mean and variance of each filter/kernel, as shown below.

- Mean: $\mu_k = (1/H \times W - 1) \sum_{i=1}^H \sum_{j=1}^W I_k ij$
- Variance: $\sigma_k^2 = (1/H \times W - 1) \sum_{i=1}^H \sum_{j=1}^W (I_k ij - \mu_k)^2$

Here, the variable k denotes the index of the layer, while H and W represent the height and width of the filter, respectively. I refers to a two-dimensional array of filters. The outcome from the statistical layer lends itself well to 1D convolution. After traversing the ensuing 1D convolutional segment, the data undergoes dynamic routing to reach the output capsules. The ultimate outcome is determined based on the activation status of the output capsules. This process is followed by the presence of five output capsules designated for the purpose of multi-class classification, depicted in Fig 5. The ultimate output is derived from the activation patterns exhibited by the output capsules.

B. Unveiling the intricacies of DF artifacts at video-level

The outcomes of each individual frame, as shown in Equation 1, after undergoing each step of frame-level fusion, are subsequently combined for the specific number of frames representing a single video instance as shown in Equation 2.

$$V_o = O_{f1}, O_{f2}, \dots, O_{fN}, \quad (2)$$

where V_o represents the output video while O_{f1}, \dots, O_{fN} represents the number of output frames from 1 upto N

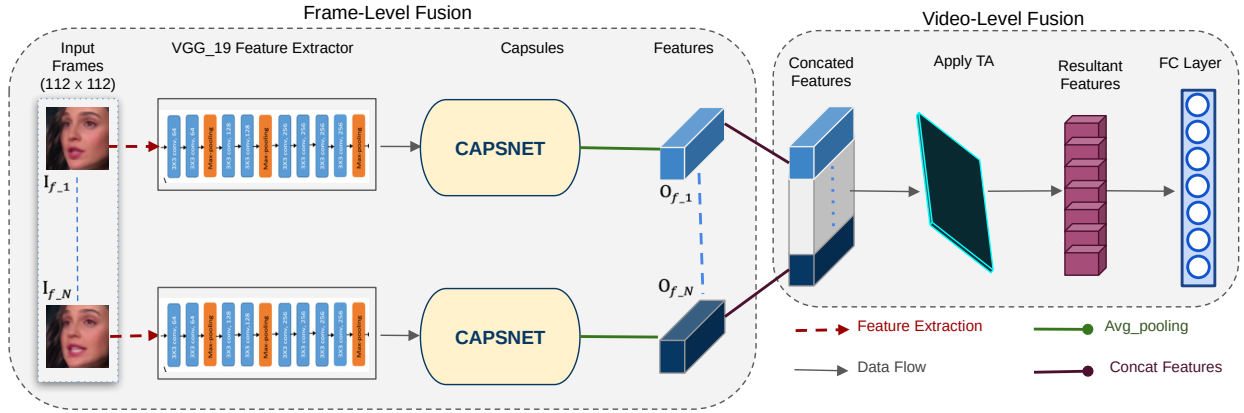


Fig. 4. An overview of CapST architecture

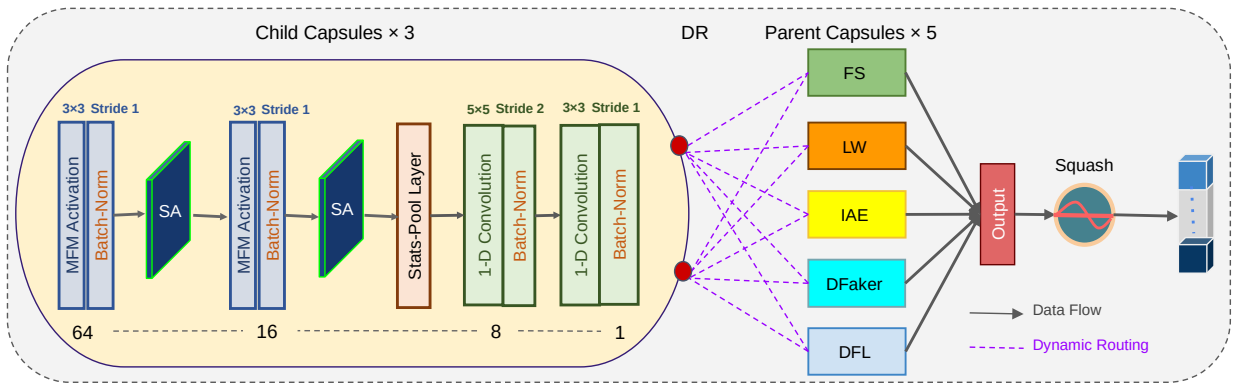


Fig. 5. Capsule Module

we chose to consider for each video. While prior research on video-level Deepfake detection mainly fused multi-frame characteristics by averaging network predictions (score fusion) [37, 25, 24, 7, 56], we have chosen to enhance classification performance by employing a temporal attention map (TAM) for adaptive feature aggregation across frames. This approach involves concatenating frame features from N faces to create multi-frame representations, which are then fused into an adaptive representation using a TAM—a structure akin to SENet [57]. The TAM utilizes the ReLU activation function along with two fully connected layers, and its output is subsequently fed into a fully connected layer for classification purposes, yielding class probabilities for the five Deepfake categories. The network is trained using the cross-entropy function. Differing from conventional Deepfake detection techniques, our approach incorporates an attention mechanism harnessing the capabilities of the Capsule Network in frame-level fusion to extract differences for model attribution subtly. In contrast to prior fingerprint-based GAN model attribution studies, the CapST takes the entire facial content as input rather than designing supplementary artifacts for multi-classification tasks, enabling effective and automatic learning of discrepancies among distinct Deepfakes.

After traversing through the stages of frame-level fusion, the outcome of each frame is amalgamated over a specific number

of frames representing an individual video. While prior investigations such as [37, 25, 24, 7, 56] in the domain of video-level Deepfake detection often amalgamated multi-frame attributes by computing an average of network predictions (score fusion), our enhancement to classification efficacy involves the deployment of a temporal attention map for the adaptive accumulation of attributes across diverse frames. Initially, the features of N faces' frames are concatenated to shape multi-frame representations, which are subsequently melded using the temporal attention map. This attention map shares a similar structure with SENet [57] and employs the ReLU activation function alongside two fully connected layers. The resulting output is then channeled through a fully connected layer tailored for classification, producing probabilities for the five Deepfake categories. Training the neural network encompasses the utilization of the cross-entropy function. In contrast to existing techniques, our strategy harnesses the attention mechanism of the Capsule Network to extract variations in model attribution at the frame level delicately. Diverging from fingerprint-based GAN model attribution studies, the CapST approach accepts entire facial content as input, obviating the need for supplementary artifacts and allowing for effective, automatic assimilation of differences among distinct Deepfakes.

Algorithm 1 CapST Algorithm

Require: Dataset of videos with N frames each
Ensure: Probabilities for each DF video's class

- 1: **for** each video V in the dataset **do**
- 2: **for** each frame I_f in N faces extracted from V **do**
- 3: Extract features from I_f using VGG_19_bn
- 4: **end for**
- 5: **for** each frame feature **do**
- 6: Pass through MFM Activation Function
- 7: Apply Batch Normalization
- 8: Pass through Spatial Attention MAP (SAM)
- 9: Compute mean (μ_k) and variance (σ_k^2) (StatsPool)
- 10: Extract final features using a 1D CNN segment
- 11: **end for**
- 12: **end for**
- 13: **Initialize:** Temporal Attention Map (TAM)
- 14: **for** each video V **do**
- 15: Concatenate features for multi-frame representations
- 16: Pass through Temporal Attention Map (TAM)
- 17: Pass through fully connected layer for classification
- 18: **end for**
- 19: **return** Class probabilities for each DF video's class

IV. EXPERIMENTS AND RESULTS

A. DFDM Dataset

The DeepFakes from Different Models (DFDM) dataset is notably pioneering within the domain of deepfakes, as highlighted by [7], owing to distinctive attributes that set it apart from other deepfake datasets. With the absence of pre-existing datasets containing labeled Deepfakes originating from diverse models, the authors introduce the novel DFDM dataset to attribute Deepfake models. Given that a majority of publicly available Deepfakes have been created utilizing Autoencoder architectures [31] [58], the study emphasizes the utilization of Autoencoder models for the generation of high-quality Deepfakes. In their investigation, they employed the widely recognized open-source software Facewap [59] in conjunction with a selection of optional DFAE models sourced from DeepFaceLab [60]. The meticulous process of choosing five models was conducted carefully, emphasizing specific criteria like utilizing the original Faceswap model as the baseline and introducing variations in components such as the encoder, decoder, intermediate layer, and input resolution. These selected models were deliberately picked to ensure subtle distinctions among the variations. A comprehensive depiction of these five models, which include Faceswap [59], Lightweight [59], IAE [59], Dfaker [61], and DFL-H128 [62], is provided in IV. It is worth noting that other models offered by Facewap consist of multiple variations amongst themselves, which are believed to be comparatively more discernible than the chosen five models within the scope of their study. Genuine videos were sourced from the Celeb-DF dataset [63], which encompasses 590 YouTube interviews featuring 59 distinct celebrities to achieve a broad spectrum of video diversity. Extraction of facial features was carried out

using the S3FD detector [64] and the FAN face aligner [65]. Each individual model underwent a training process spending 100,000 iterations, culminating in the production of Deepfake videos in MPEG4.0 format. The generation process considered three different H.264 compression rates to yield videos of varying quality: a lossless option with a constant rate factor (CRF) of 0, a high-quality variant with a CRF of 10, and a low-quality version with a CRF of 23. Collectively, a total of 6,450 Deepfakes were synthesized. A set of facial illustrations is displayed in Figure 3, showcasing instances of Deepfakes produced by the five models using the same training dataset. Evident dissimilarities within facial regions underscore the presence of artifacts that can be attributed to specific models.

B. Experimental Setting

Before conducting our experiments, we divided the DFDM dataset into training and testing sets following the guidelines provided by [7], with a ratio of 70% for training and 30% for testing. To extract frames from each video in the dataset, we utilized the OpenFace open-source library [66], known for its accuracy and reliability. The extracted frames were saved in PNG format with a dimension of 112×112 pixels. By using a lower dimension, we aimed to reduce the computational resources required for training our model, which is one of the main objectives of this study. To ensure a balanced distribution of faces in frame selection, we employed periodic sampling to select 10 frames from each video for our proposed approach. Our experimental results indicate a clear performance improvement when increasing the number of frames from 1 to 10, while the performance becomes stable beyond 10 frames. Thus, the network takes the cropped faces with dimensions of $112 \times 112 \times 3 \times 10$ as input. For training the network, we used the SGD optimizer with a weight decay of 5×10^{-4} and a momentum of 0.9. The learning rate was set to 0.01 throughout the entire training process. A batch size of 10 was employed, and the training was conducted for 300 epochs.

C. Results Comparison With Existing Methods

Table V compares our model and various state-of-the-art methods, including attention-based and other classification approaches. Our model stands out, surpassing all other contenders in terms of overall accuracy. This success underscores the superior classification prowess of our approach. While some of the competing models leverage skip connections and more intricate architectures, our choice of a simple VGG19_bn model without residuals yields exceptional results. These models may exhibit enhanced performance in specific classes due to their utilization of models that uses skip connections, which can sometimes perform better in specific condition/classes, but their overall effectiveness falls short of overall improvement. It's important to acknowledge that, in general, ResNet has demonstrated superior accuracy compared to VGG19_bn across diverse image recognition tasks, particularly on large-scale challenges like ImageNet. However, for our specific

TABLE V
COMPARISON OF CAPST MODEL WITH DIFFERENT METHODS (ACC%). THE BEST SCORE IS MARKED IN BOLD.

Method	FaceSwap	LightWeight	IAE	Dfaker	DFL-H128	Average
MesoInception [25]	6.98	2.33	79.07	79.07	4.65	20.93
XceptionNet [21]	0.77	0.00	12.40	12.40	19.38	20.93
R3D [67]	27.13	25.58	15.5	20.16	18.61	21.40
DnCNN [50]	2.33	0.00	0.00	7.75	99.22	21.86
DSP-FWA [37]	17.05	7.75	43.41	40.31	8.87	23.41
GAN Fingerprint [48]	20.16	22.48	54.26	21.71	26.36	28.99
DFT-spectrum [68]	99.92	3.26	0.23	27.21	48.91	35.91
Capsule [24]	32.56	42.64	69.77	73.64	58.91	55.50
SAM+FA [69]	64.34	42.64	76.61	74.42	79.07	66.82
ResNet-50 [70]	54.84	57.36	70.54	89.92	70.54	68.02
CBAM [55]	52.42	63.57	69.77	84.50	74.42	68.53
SAM+Ave	58.87	51.16	76.74	80.62	79.07	68.84
DMA-STA [7]	63.57	58.91	66.67	82.95	87.60	71.94
CapST[Ours]	77.69	53.84	60.76	93.07	92.30	75.54

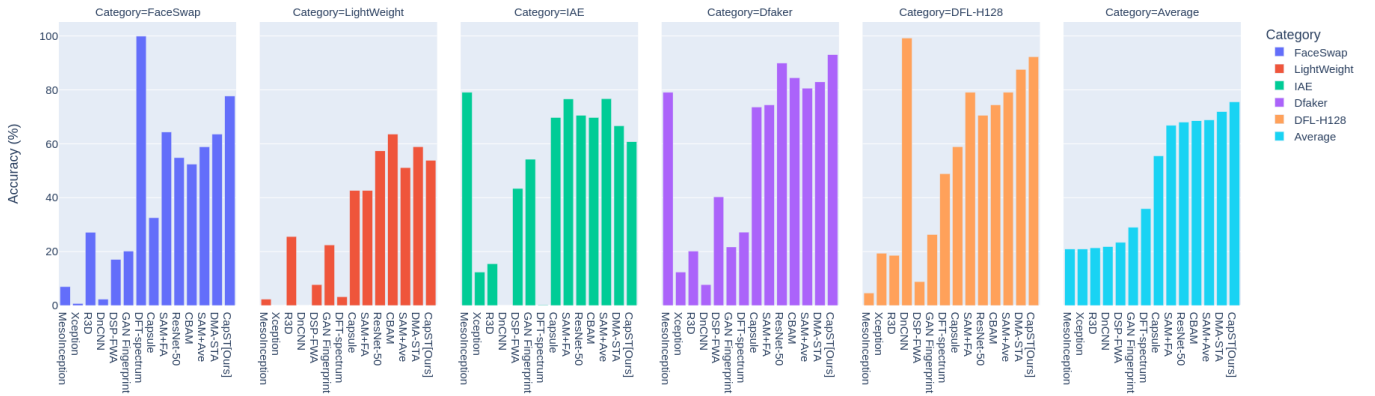


Fig. 6. Results Comparison of CapST Model Against Existing Methods

problem domain and dataset, VGG19_bn has proven to be a robust performer. Ultimately, the decision to opt for ResNet or VGG19_bn should be made thoughtfully, considering the specific demands and nuances of each task at hand. To conclude, we carefully conducted several experiments and observed that VGG_19_bn, combined with Capsule Network, can achieve better performance, as shown in Figure 6.

D. Comparing Our Results to DMA-STA Reproduced Results

While the initial performance of DMA-STA [7] was promising, our model demonstrated significant superiority after applying our custom settings, as shown in Table VI. However, we have difficulty replicating their outcomes using their GitHub repository’s experimental configurations. Our machine’s limited GPU memory prevented us from using their settings. To optimize model efficiency and resource usage, we adjusted the original settings that involved image dimensions from the video dataset and batch size. The original DMA-STA experiments employed Titan XP GPUs [71], but we had access to a single GPU with 12 Gigabytes of memory. To ensure a fair comparison, we adapted the experimental parameters to reproduce DMA-STA’s results on our machine. Specifically, we reduced image dimensions from 300×300 to 112×112 and the batch size from 20 to 10 while keeping other settings

unchanged. For a detailed explanation of the rationale behind these adjustments, please refer to Section V-A.

E. Parameters Comparison with DMA-STA

Incorporating ResNet for feature extraction, renowned for its efficient parameter utilization, the DMA-STA network takes a step further by integrating two modules known as Spatial-Temporal attention. In the initial segment of these modules,

TABLE VI
COMPARISON WITH DMA-STA REPRODUCED RESULTS. THE BEST SCORE IS MARKED IN BOLD.

Method	lr	FS	LW	IAE	Dfaker	DFL	Avg
DMA-STA* citejia2022model	0.01	53.84	48.46	61.53	76.92	63.84	60.92
CapST: Orig_Caps	0.0001	70.00	40.00	73.07	90.00	83.84	71.53
CapST: Orig_Caps	0.01	72.30	38.46	76.92	87.69	91.53	73.38
CapST: MFM_5×5	0.01	72.30	42.30	73.84	90.76	91.53	74.15
CapST: MFM_3×3	0.01	77.69	53.84	60.76	93.07	92.30	75.54

¹ DMA-STA* reproduced results of the baseline method on our hardware.

² lr, FS, LW and DFL represent Learning Rate, FaceSwap, Lightweight and DFL-H128, respectively

³ 5×5 and 3×3 are kernel sizes

TABLE VII
PARAMETERS AND TRAINING TIME COMPARISON OF DMA-STA AND
CAPST MODELS ON RTX-3080TI

Index	Model Layers	Params(Millions)	Training Time(Minutes)
DMA-STA [7]			
0	Conv2D	9408	0.5025 × 300
1	BatchNorm	128	
2	Layer 1-4	23500064	
3	TA-FC0	50	
4	TA-FC1	50	
5	TA-FC	10245	
Total		23.52	150.75
CapsT [Ours]			
0	VGG	2328330	0.373 × 300
1	CapsNet×3	942027	
2	TA-FC0	50	
3	TA-FC1	50	
4	TA-FC	2565	
Total		3.273	

¹ Training Time* is calculated for 300 epochs in each experiment, as mentioned in the table above.

frame-level characteristics are derived from N cropped faces via the utilization of the Spatial Attention Map (SAM). This process inherently captures elevated-level representations, facilitated by utilizing the lightweight and versatile convolutional block attention module introduced by [55]. Moreover, the Temporal Attention Map (TAM) is harnessed to adaptively consolidate attributes from diverse frames. Integrating these intricate modules leads to a substantial augmentation in the model’s parameter count, culminating in a total of 23.520 million parameters. In contrast, our model not only surpasses the performance of the existing one but also significantly reduces the number of parameters to a mere 3.27 million, which is almost eight times smaller than the current model’s parameter count. We also consider training time an essential factor, as training huge models that require substantial time for learning data might be undesirable in the future. Therefore, we have designed our model to take less time to train while still outperforming existing models in this specific task, as demonstrated in Table VII. This approach ensures efficiency in training without compromising performance.

V. DISCUSSION

The CapST module’s robust capabilities extend beyond mere computational resource reduction, encompassing the simultaneous maintenance of high performance. Our approach unfolds in four distinct phases. Initially, frames are extracted from each video. Subsequently, these frames are subjected to feature extraction using the VGG19_bn model. The decision to favor VGG19_bn over ResNet stems from its demonstrated superior performance when integrated with the Capsule network, a conclusion drawn from meticulous experimentation involving both architectures. Notably, despite ResNet’s intrinsic parameter efficiency compared to VGG19_bn, a deliberate choice is made to exclusively engage the first three Maxpooling layers of VGG19_bn (which spans 26 layers), effectively constraining the overall parameter count during the training process. Moving forward, the extracted features are channeled into the Capsule module, enriching each input

TABLE VIII
RESOURCES AND PERFORMANCE COMPARISON OF CAPST MODEL
AGAINST DIFFERENT MODELS (ACC%). THE BEST ONE IS MARKED
IN BOLD.

Model	Training Time	Params	Avg: Acc(%)
MobileNet-V1 [1]	33	3.21	21.69
EfficientNet [2]	90	4.01	71.69
ResNet-50 [70]	116	23.52	60.92
ResNet-101 [70]	203	42.51	60.61
ResNet-152 [70]	268	57.03	60.46
XceptionNet [73]	120	20.81	38.61
InceptionNet [74]	126	6.27	42.76
MobileNet-V2 [72]	118	2.23	21.69
CapST[Ours]	112	3.27	75.54

¹ Training Time* is presented in Minutes.

² Parameters* are presented in Millions

video frame with spatial characteristics. Lastly, the video-level fusion procedure comes into play, culminating in successfully classifying the video into its pertinent category of interest. The distinguishing factor between CapST and prior studies lies in our deliberate efforts to reduce image dimensions, batch size, and training time. These considerations, tailored to the constraints of FPGA-based hardware, yield a substantial solution to address the challenge of classifying deepfake content. Further elaboration is provided in Section V-A.

A. Ablation Study

We made several modifications to the baseline model aimed at reducing computational demands while simultaneously enhancing performance in video classification, as illustrated in Table VIII. To evaluate the efficacy of these changes, we substituted the Capsule Network with various existing models, carrying out these experiments under uniform settings and environmental conditions. For every experiment, the input frame dimensions were fixed at 112×112 , and we opted for a batch size of 10 for both the training and testing phases. This choice was due to hardware limitations that restricted us from employing batch sizes greater than 10. Each experiment was executed for 300 epochs, and the results were analyzed. As depicted in Figure 7, MobileNet [1] exhibited the shortest training time of 33 minutes and a relatively low parameter count of 3.21 million during the training process. However, its performance was notably low, registering at 21.69%. Similarly, MobileNet-V2 [72] possessed fewer training parameters, yet its training time was comparatively higher, and its performance is the same as that of MobileNet [1], which was subpar. EfficientNet [2] achieved a relatively higher performance score of 71.69%, supported by a modest training parameter count of 4.01 million and a training duration of 90 minutes. However, compared to our proposed model, its overall performance remains inferior. Compared to all other models, our proposed model exhibited an appropriate training time and an impressively lower parameter count, outperforming all others. This model’s performance also surpassed that of its counterparts. The rationale underpinning these modifications is elaborated upon in the subsequent explanation.

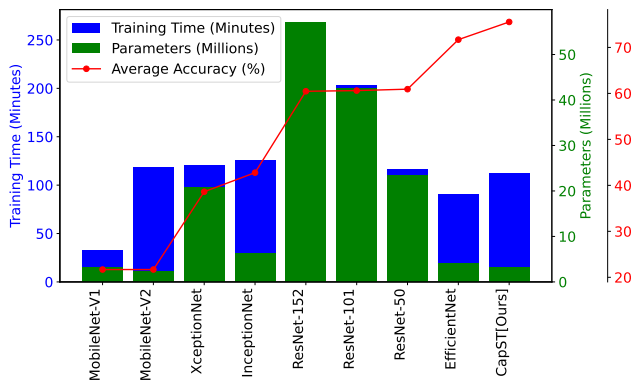


Fig. 7. Resources/Performance Comparison of CapST and Existing Models on DFDM Dataset

B. Discussions

1) *Dimension of Images:* The dimension of images in a dataset can significantly impact the model size, especially in deep learning architectures. The model size mainly depends on the number of parameters it needs to learn to represent the data effectively. Here is how the dimension of images can influence the model size.

Pixels Impact: Image dimension directly affects pixel count. Larger images demand more parameters to process, e.g., 256×256 vs. 64×64 .

Convolutional Layers: Input image size determines convolutional layer dimensions in architectures like CNNs. Larger images might need more filters, increasing parameters.

Fully Connected Layers: Image size affects units in dense layers. Larger images may need more units, leading to increased parameters.

Pooling Layers: Larger images may require additional pooling layers, impacting model size by reducing spatial dimensions.

Memory Needs: Larger images demand more memory for model weights and activations, affecting the model's feasibility.

Computational Costs: Processing larger images increases floating-point operations, extending training and inference times.

Optimal Image Dimensions: Balance between model size and detail is crucial. Excessive reduction can lead to loss of vital information, affecting model performance.

To conclude, smaller image dimensions cut parameters, memory, and costs. But balance is key; overly reducing size may lose vital details, harming the model's performance. Deciding on image dimensions requires careful consideration of the trade-offs between size and performance in deep-learning tasks.

2) *Effect of Batch size:* The best choice of batch size depends on various factors, including the specific deep learning

task, available hardware resources, and the dataset size. There is no one-size-fits-all answer, and the optimal batch size may vary from one scenario to another. However, it has some effects as follows.

Training Efficiency: Larger batch sizes accelerate training, processing more samples in parallel on GPUs. Smaller batches take longer but can converge to better solutions with fewer iterations.

Generalization: Large batch sizes may overfit and converge to suboptimal minima. Small batches act as regularization, enhancing generalization, crucial for small datasets.

Hardware Constraints: Large batches demand more memory, challenging on limited GPU/system memory. Small batches are memory-efficient, ideal for systems with restricted resources and transfer learning scenarios.

Batch Noise: Large batches smooth noisy data, while smaller batches escape bad minima, exploring the loss landscape effectively. Choose based on your specific needs and resources.

Experimenting with batch sizes is common. Balance efficiency and generalization by monitoring progress and resources. Larger batches are speedy for big datasets and ample hardware, while smaller batches enhance generalization, vital for limited resources. For our dataset and limited hardware, we opted for a smaller batch size in our experiments.

3) *Effect of Training Time:* Training time is another crucial factor in deep neural networks for several reasons, and saving time during training can have significant implications. Here are some reasons why training time matters and how it impacts the development and usage of deep neural networks:

Reduced Computational Cost: Faster training cuts expenses, vital for expensive GPUs and cloud platforms.

Iterative Improvements: Speedier training enables more iterations, fostering gradual enhancements for optimal performance.

Rapid Prototyping: Faster training allows swift testing, identifying promising approaches during architecture prototyping.

Hyperparameter Tuning: Speedy training streamlines fine-tuning, pivotal for deep neural network success.

Deployment and Production: Quicker training accelerates model updates for real-world operational use.

Resource Allocation: Limited resources benefit from shorter training, enabling parallel training or quicker model iterations.

Research Scale: Reduced training times enhance broad experiments, expanding exploration possibilities.

Time-Sensitive Applications: Swift training ensures responsiveness in real-time systems, crucial for predictive and decision-making contexts.

Maintaining quality while achieving faster training is crucial. Balance between efficiency and accuracy is key. Tech-

niques like efficient architectures, hyperparameter optimization, and hardware accelerators help. The right balance depends on the specific use case and resources.

4) *Effect of parameters on FPGA(Field-Programmable Gate Array) hardware:* The number of parameters in a Deep Learning model has a significant effect on FPGA (Field-Programmable Gate Array) hardware in terms of various aspects:

Resource Utilization: Large models strain FPGA resources, impacting on-chip and external memory use.

Model Deployment: Model size affects FPGA deployment in resource-constrained edge devices.

Latency and Throughput: Parameter count influences computation time, affecting FPGA system throughput.

Power Consumption: More parameters increase FPGA power usage, impacting energy efficiency.

Model Parallelism: FPGA parallelism depends on model size and available resources.

Model Update Frequency: Many parameters can slow FPGA reprogramming for responsive systems.

Memory Bandwidth: Large models demand high memory bandwidth, requiring FPGA memory optimizations.

Training on FPGAs: Larger models extend FPGA training time, posing scalability concerns.

Quantization and Compression: Techniques like quantization and compression shrink models for FPGA fit.

Optimizing Deep Learning models for FPGA deployment involves striking a balance between model complexity, resource constraints, and performance requirements. Efficient model design, pruning, quantization, and hardware-aware optimization techniques are essential to harness the full potential of FPGA-based Deep Learning accelerators.

VI. CONCLUSION

In conclusion, this study presents a novel, lightweight, optimized model for accurately classifying deepfake videos using five different encoders. By leveraging a Convolutional Neural Network (CNN) as the backbone for efficient feature extraction and incorporating a Capsule Network (CapsNet) as a spatial attention mechanism, our model achieves robust identification of deepfake attributes. Additionally, introducing video-level fusion as a temporal attention mechanism allows our model to exploit temporal dependencies, leading to more accurate predictions. Experimental results on a large-scale benchmark dataset of deepfake videos demonstrate the effectiveness and superiority of our proposed approach, showcasing significantly improved performance compared to the baseline model while reducing computational costs. As the threat of deepfake videos grows in various domains, our approach provides a valuable solution for enhanced deepfake detection and prevention.

VII. ACKNOWLEDGEMENTS

This work was supported in part by National Science and Technology Council under grant nos. 112-2223-E-001-001, 111-2221-E-001-013-MY3, 111-2923-E-002-014-MY3, and 112-2927-I-001-508 and Academia Sinica under grant no. AS-IA-111-M01.

REFERENCES

- [1] Andrew G Howard et al. “Mobilenets: Efficient convolutional neural networks for mobile vision applications”. In: *arXiv preprint arXiv:1704.04861* (2017).
- [2] Mingxing Tan and Quoc Le. “Efficientnet: Rethinking model scaling for convolutional neural networks”. In: *International conference on machine learning*. PMLR, 2019, pp. 6105–6114.
- [3] Xiangyu Zhang et al. “Shufflenet: An extremely efficient convolutional neural network for mobile devices”. In: *Proceedings of the IEEE conference on computer vision and pattern recognition*. 2018, pp. 6848–6856.
- [4] Han Cai, Ligeng Zhu, and Song Han. “Proxylessnas: Direct neural architecture search on target task and hardware”. In: *arXiv preprint arXiv:1812.00332* (2018).
- [5] Hieu Pham et al. “Efficient neural architecture search via parameters sharing”. In: *International conference on machine learning*. PMLR, 2018, pp. 4095–4104.
- [6] Barret Zoph and Quoc V Le. “Neural architecture search with reinforcement learning”. In: *arXiv preprint arXiv:1611.01578* (2016).
- [7] Shan Jia, Xin Li, and Siwei Lyu. “Model attribution of face-swap deepfake videos”. In: *2022 IEEE International Conference on Image Processing (ICIP)*. IEEE, 2022, pp. 2356–2360.
- [8] Ian Goodfellow, Yoshua Bengio, and Aaron Courville. *Deep learning*. MIT press, 2016.
- [9] Alex Krizhevsky, Ilya Sutskever, and Geoffrey E Hinton. “Imagenet classification with deep convolutional neural networks”. In: *Communications of the ACM* 60.6 (2017), pp. 84–90.
- [10] Karen Simonyan and Andrew Zisserman. “Very deep convolutional networks for large-scale image recognition”. In: *arXiv preprint arXiv:1409.1556* (2014).
- [11] Yann LeCun, Yoshua Bengio, and Geoffrey Hinton. “Deep learning”. In: *nature* 521.7553 (2015), pp. 436–444.
- [12] Li Deng, Dong Yu, et al. “Deep learning: methods and applications”. In: *Foundations and trends® in signal processing* 7.3–4 (2014), pp. 197–387.
- [13] Vivienne Sze et al. “Efficient processing of deep neural networks: A tutorial and survey”. In: *Proceedings of the IEEE* 105.12 (2017), pp. 2295–2329.
- [14] Song Han et al. “Learning both weights and connections for efficient neural network”. In: *Advances in neural information processing systems* 28 (2015).

- [15] Ilija Radosavovic et al. "Designing network design spaces". In: *Proceedings of the IEEE/CVF conference on computer vision and pattern recognition*. 2020, pp. 10428–10436.
- [16] Pavlo Molchanov et al. "Pruning convolutional neural networks for resource efficient inference". In: *arXiv preprint arXiv:1611.06440* (2016).
- [17] Yu Cheng et al. "A survey of model compression and acceleration for deep neural networks". In: *arXiv preprint arXiv:1710.09282* (2017).
- [18] Chenzhuo Zhu et al. "Trained ternary quantization". In: *arXiv preprint arXiv:1612.01064* (2016).
- [19] Jiwen Lu et al. "Learning compact binary face descriptor for face recognition". In: *IEEE transactions on pattern analysis and machine intelligence* 37.10 (2015), pp. 2041–2056.
- [20] Simon Wu et al. "Distilled vision transformer". In: (2020). This paper is not available.
- [21] Andreas Rossler et al. "Faceforensics++: Learning to detect manipulated facial images". In: *Proceedings of the IEEE/CVF international conference on computer vision*. 2019, pp. 1–11.
- [22] Burak Bekci, Zahid Akhtar, and Hazim Kemal Ekenel. "Cross-dataset face manipulation detection". In: *2020 28th Signal Processing and Communications Applications Conference (SIU)*. IEEE. 2020, pp. 1–4.
- [23] Mingyu Ding et al. "Hr-nas: Searching efficient high-resolution neural architectures with lightweight transformers". In: *Proceedings of the IEEE/CVF Conference on Computer Vision and Pattern Recognition*. 2021, pp. 2982–2992.
- [24] Huy H Nguyen, Junichi Yamagishi, and Isao Echizen. "Capsule-forensics: Using capsule networks to detect forged images and videos". In: *ICASSP 2019-2019 IEEE International Conference on Acoustics, Speech and Signal Processing (ICASSP)*. IEEE. 2019, pp. 2307–2311.
- [25] Darius Afchar et al. "Mesonet: a compact facial video forgery detection network". In: *2018 IEEE international workshop on information forensics and security (WIFS)*. IEEE. 2018, pp. 1–7.
- [26] Xiaoming Li et al. "Blind face restoration via deep multi-scale component dictionaries". In: *Computer Vision–ECCV 2020: 16th European Conference, Glasgow, UK, August 23–28, 2020, Proceedings, Part IX 16*. Springer. 2020, pp. 399–415.
- [27] Ziwei Liu et al. "Deep learning face attributes in the wild". In: *Proceedings of the IEEE international conference on computer vision*. 2015, pp. 3730–3738.
- [28] B Dolhansky et al. "The DeepFake detection challenge dataset.(2020)". In: *ArXiv: abs* (2006).
- [29] Justus Thies et al. "Face2face: Real-time face capture and reenactment of rgb videos". In: *Proceedings of the IEEE conference on computer vision and pattern recognition*. 2016, pp. 2387–2395.
- [30] Arsha Nagrani, Joon Son Chung, and Andrew Senior. "Voxceleb: a large-scale speaker identification dataset". In: *arXiv preprint arXiv:1706.08612* (2017).
- [31] Brian Dolhansky et al. "The deepfake detection challenge (dfdc) preview dataset". In: *arXiv preprint arXiv:1910.08854* (2019).
- [32] Lingzhi Li et al. "Face x-ray for more general face forgery detection". In: *Proceedings of the IEEE/CVF conference on computer vision and pattern recognition*. 2020, pp. 5001–5010.
- [33] Alexandros Haliassos et al. "Lips don't lie: A generalisable and robust approach to face forgery detection". In: *Proceedings of the IEEE/CVF conference on computer vision and pattern recognition*. 2021, pp. 5039–5049.
- [34] Yinglin Zheng et al. "Exploring temporal coherence for more general video face forgery detection". In: *Proceedings of the IEEE/CVF international conference on computer vision*. 2021, pp. 15044–15054.
- [35] Du Tran et al. "Video classification with channel-separated convolutional networks". In: *Proceedings of the IEEE/CVF International Conference on Computer Vision*. 2019, pp. 5552–5561.
- [36] Peng Zhou et al. "Two-stream neural networks for tampered face detection". In: *2017 IEEE conference on computer vision and pattern recognition workshops (CVPRW)*. IEEE. 2017, pp. 1831–1839.
- [37] Yuezun Li and Siwei Lyu. "Exposing DeepFake Videos By Detecting Face Warping Artifacts". In: *IEEE Conference on Computer Vision and Pattern Recognition Workshops (CVPRW)*. 2019.
- [38] Hanqing Zhao et al. "Multi-attentional deepfake detection". In: *Proceedings of the IEEE/CVF conference on computer vision and pattern recognition*. 2021, pp. 2185–2194.
- [39] Wasim Ahmad et al. "ResViT: A Framework for Deepfake Videos Detection". In: *International journal of electrical and computer engineering systems* 13.9 (2022), pp. 807–813.
- [40] Davide Alessandro Coccomini et al. "Combining efficientnet and vision transformers for video deepfake detection". In: *Image Analysis and Processing–ICIAP 2022: 21st International Conference, Lecce, Italy, May 23–27, 2022, Proceedings, Part III*. Springer. 2022, pp. 219–229.
- [41] Young-Jin Heo et al. "Deepfake detection scheme based on vision transformer and distillation". In: *arXiv preprint arXiv:2104.01353* (2021).
- [42] Selim Seferbekov. *DFDC 1st place solution*. 2020.
- [43] Deressa Wodajo and Solomon Atnafu. "Deepfake video detection using convolutional vision transformer". In: *arXiv preprint arXiv:2102.11126* (2021).
- [44] Sahibzada Adil Shahzad et al. "Lip Sync Matters: A Novel Multimodal Forgery Detector". In: *2022 Asia-Pacific Signal and Information Processing Association Annual Summit and Conference (APSIPA ASC)*. IEEE. 2022, pp. 1885–1892.
- [45] Ammarah Hashmi et al. "Multimodal Forgery Detection Using Ensemble Learning". In: *2022 Asia-Pacific Signal and Information Processing Association Annual Summit and Conference (APSIPA ASC)*. 2022, pp. 1524–1532. DOI: 10.23919/APSIPAASC55919.2022.9980255.

- [46] Sharath Girish et al. "Towards discovery and attribution of open-world gan generated images". In: *Proceedings of the IEEE/CVF International Conference on Computer Vision*. 2021, pp. 14094–14103.
- [47] Ning Yu, Larry S Davis, and Mario Fritz. "Attributing fake images to gans: Learning and analyzing gan fingerprints". In: *Proceedings of the IEEE/CVF international conference on computer vision*. 2019, pp. 7556–7566.
- [48] Francesco Marra et al. "Do gans leave artificial fingerprints?" In: *2019 IEEE conference on multimedia information processing and retrieval (MIPR)*. IEEE. 2019, pp. 506–511.
- [49] Michael Goebel et al. "Detection, attribution and localization of gan generated images". In: *arXiv preprint arXiv:2007.10466* (2020).
- [50] Vishal Asnani et al. "Reverse engineering of generative models: Inferring model hyperparameters from generated images". In: *arXiv preprint arXiv:2106.07873* (2021).
- [51] Olga Russakovsky et al. "Imagenet large scale visual recognition challenge". In: *International journal of computer vision* 115 (2015), pp. 211–252.
- [52] Xiang Wu et al. "A light CNN for deep face representation with noisy labels". In: *IEEE Transactions on Information Forensics and Security* 13.11 (2018), pp. 2884–2896.
- [53] Nicolas Rahmouni et al. "Distinguishing computer graphics from natural images using convolution neural networks". In: *2017 IEEE workshop on information forensics and security (WIFS)*. IEEE. 2017, pp. 1–6.
- [54] Huy H Nguyen et al. "Modular convolutional neural network for discriminating between computer-generated images and photographic images". In: *Proceedings of the 13th international conference on availability, reliability and security*. 2018, pp. 1–10.
- [55] Sanghyun Woo et al. "Cbam: Convolutional block attention module". In: *Proceedings of the European conference on computer vision (ECCV)*. 2018, pp. 3–19.
- [56] Jiaming Li et al. "Frequency-aware discriminative feature learning supervised by single-center loss for face forgery detection". In: *Proceedings of the IEEE/CVF conference on computer vision and pattern recognition*. 2021, pp. 6458–6467.
- [57] Jie Hu, Li Shen, and Gang Sun. "Squeeze-and-excitation networks". In: *Proceedings of the IEEE conference on computer vision and pattern recognition*. 2018, pp. 7132–7141.
- [58] Bojia Zi et al. "Wilddeepfake: A challenging real-world dataset for deepfake detection". In: *Proceedings of the 28th ACM international conference on multimedia*. 2020, pp. 2382–2390.
- [59] deepfakes. *Faceswap*. <https://github.com/deepfakes/faceswap>. 2017.
- [60] iperov. *DeepFaceLab*. <https://github.com/iperov/DeepFaceLab>. 2020.
- [61] Dfaker. *DepFA*. <https://github.com/dfaker/df>. 2020.
- [62] Ivan Perov et al. "DeepFaceLab: Integrated, flexible and extensible face-swapping framework". In: *arXiv preprint arXiv:2005.05535* (2020).
- [63] Yuezun Li et al. "Celeb-df: A large-scale challenging dataset for deepfake forensics". In: *Proceedings of the IEEE/CVF conference on computer vision and pattern recognition*. 2020, pp. 3207–3216.
- [64] Shifeng Zhang et al. "S3fd: Single shot scale-invariant face detector". In: *Proceedings of the IEEE international conference on computer vision*. 2017, pp. 192–201.
- [65] Adrian Bulat and Georgios Tzimiropoulos. "How far are we from solving the 2d & 3d face alignment problem?(and a dataset of 230,000 3d facial landmarks)". In: *Proceedings of the IEEE international conference on computer vision*. 2017, pp. 1021–1030.
- [66] Tadas Baltrusaitis et al. "Openface 2.0: Facial behavior analysis toolkit". In: *2018 13th IEEE international conference on automatic face & gesture recognition (FG 2018)*. IEEE. 2018, pp. 59–66.
- [67] Oscar De Lima et al. "Deepfake detection using spatiotemporal convolutional networks". In: *arXiv preprint arXiv:2006.14749* (2020).
- [68] Ricard Durall et al. "Unmasking deepfakes with simple features". In: *arXiv preprint arXiv:1911.00686* (2019).
- [69] Debin Meng et al. "Frame attention networks for facial expression recognition in videos". In: *2019 IEEE international conference on image processing (ICIP)*. IEEE. 2019, pp. 3866–3870.
- [70] Kaiming He et al. "Deep residual learning for image recognition". In: *Proceedings of the IEEE conference on computer vision and pattern recognition*. 2016, pp. 770–778.
- [71] shanface33. *Deepfake Model Attribution Issue 2*. https://github.com/shanface33/Deepfake_Model_Attribution/issues/2. Accessed: May 11, 2023. 2023.
- [72] Mark Sandler et al. "Mobilenetv2: Inverted residuals and linear bottlenecks". In: *Proceedings of the IEEE conference on computer vision and pattern recognition*. 2018, pp. 4510–4520.
- [73] François Chollet. "Xception: Deep learning with depth-wise separable convolutions". In: *Proceedings of the IEEE conference on computer vision and pattern recognition*. 2017, pp. 1251–1258.
- [74] Christian Szegedy et al. "Going deeper with convolutions". In: *Proceedings of the IEEE conference on computer vision and pattern recognition*. 2015, pp. 1–9.



Wasim Ahmad received his bachelor's degree in computer science from Abdul Wali Khan University Mardan, Pakistan, in 2013. He then completed his master's degree in System and Software Engineering from National Research University HSE, Moscow, Russia, in 2018. He is currently pursuing PhD under the TIGP at the Institute of Information Science, Academia Sinica, in collaboration with National Chengchi University, Taipei, Taiwan. His research interests include AI-Multimedia Forgery Detection, Computer Vision, Image Processing and NLP.



Sahibzada Adil Shahzad received a B.S. degree in Software Engineering from the University of Science and Technology Bannu, Pakistan, in 2016, and an M.S. degree in computer science from the Beijing Institute of Technology, China in 2019. He is currently pursuing a Ph.D. degree with the Taiwan International Graduate Program in Social Networks and Human-Centered Computing, Institute of Information Science, Academia Sinica, Taipei, Taiwan, and the Department of Computer Science, Faculty of Science, National Chengchi University, Taipei, Taiwan. His research interests include machine learning, multimedia forensics, and image, video, and audio processing.



Yuan-Hao Chang (Fellow, IEEE) received his Ph.D. in Computer Science from the Department of Computer Science and Information Engineering at National Taiwan University, Taipei, Taiwan. He is currently a Research Fellow at the Institute of Information Science, Academia Sinica, Taipei, Taiwan. His research interests include memory/storage systems, operating systems, embedded systems, and real-time systems. He is a Fellow of IEEE.



Yan-Tsung Peng (Member, IEEE) received the Ph.D. degree in electrical and computer engineering from the University of California, San Diego, in 2017. In 2019, he joined the National Chengchi University, where he is currently an Assistant Professor in the Department of Computer Science. Before that, he was a Senior Engineer with Qualcomm Technologies, Inc., San Diego, CA, USA. His research interests include image processing, video compression, and machine-learning applications.



Gaddisa Olani Ganfure is currently an Assistant Professor of Computer Science at Dire Dawa University, Ethiopia. He received his bachelor's and master's degrees in computer science from Wollolega University and Addis Ababa University, respectively, and his Ph.D. in Social Network Analysis and Human-Centered Computing from National Tsing Hua University in collaboration with Academia Sinica, Taiwan. His research interests include cybersecurity, artificial intelligence, and natural language processing. He has received three national patents

and published numerous papers in top-tier computer science journals.



Sarwar Khan received the BSC degree in Telecommunication Engineering from University of Engineering and Technology Peshawar, Pakistan in 2011 and ME degree in Information and Communication Technology from Kasetsart University, Thailand., in 2017. He is currently pursuing a Ph.D degree in social networks and human-centered computing with CITI, Academia Sinica. His research interests include deep learning, computer vision, and multimedia.